Proposal for the temperature–electric-field phase diagram of a ferroelectric smectic-*C** liquid crystal

F. Ghoddoussi,[1] M. A. Pantea,[1] P. H. Keyes,[1] R. Naik,[1] and P. P. Vaishnava[2]
[1]*Department of Physics and Astronomy, Wayne State University, Detroit, Michigan 48202, USA*
[2]*Department of Science and Mathematics, Kettering University, Flint, Michigan 48504, USA*
(Received 9 July 2003; published 25 November 2003)

We report on the results of extensive optical measurements on the ferroelectric smectic-*C** phase of the chiral liquid crystal 4-(2′ methyl butyl) phenyl 4′-*n*-octylbiphenyl-4-carboxylate. We have explored the entire temperature–electric-field phase space searching for all possible phase transitions in the *C** region and have characterized them both as to their character, including whether they are first or second order, and also whether they are of instability or nucleation type. Our results lead us to conclude that the experimental phase diagram is incompatible with all existing theoretical models for the *C** phase transitions. We propose instead a phase diagram where two second-order lines and one first-order line meet at a triple point that we tentatively identify as a Lifshitz point.

DOI: 10.1103/PhysRevE.68.051706 PACS number(s): 61.30.Eb, 61.30.Gd

INTRODUCTION

The smectic-*C** phase is the smectic-*C* phase formed by optically active molecules. In the *C** phase the direction of molecular tilt is not uniform as it is in the *C* phase, but instead precesses along an axis perpendicular to the smectic layers. The structure repeats along the helical axis in a distance P, the pitch, and associated with this is a wave vector $q=2\pi/P$. The *C** phase is therefore a twisted or helicoidal phase reminiscent of the cholesteric or *N** phase, a major difference being that the molecules are perpendicular to the twist axis in an *N** phase whereas in the *C** phase they make a smaller angle θ, which is the (temperature dependent) tilt angle. Meyer *et al.* [1] realized through symmetry arguments that such a structure must have a net polarization perpendicular to the local tilt plane. The *C** phase is thus one of the only examples of a ferroelectric, or more properly helielectric, liquid crystal.

The response of a *C** phase to an electric field has obviously been a subject of central importance, which, as it turns out, has had a long and tortuous history. Despite the many revisions that have taken place over the years, there has still not been a convergence between the theoretical predictions and the experiments, in our viewpoint. The first half of this paper will outline the history of this subject, emphasizing these failures, while the second half will present what the experiments suggest to be the correct situation.

The phase diagram of a *C** phase in the presence of a dc electric field was initially thought to be rather simple [2]. The second-order *A**-*C** transition that takes place in zero field is shifted downward in temperature upon application of the field, which also changes the symmetries of the two phases somewhat. The higher-temperature *A** phase tilts under the application of the field (the electroclinic effect) and thus becomes a $\overline{C^*}$ phase, a *uniform*, tilted, nonhelicoidal phase. The only order parameter associated with the $\overline{C^*}$ phase is the magnitude of the tilt angle. The *C** phase becomes a *distorted, nonuniform* helicoidal phase when the field is on. For low enough fields its structure may be thought to consist of two terms: a sinusoidal helix plus a uniform tilt. Associated with the *C** phase then are *two* order parameters, one the amplitude of the helicoidal component, and the other the amplitude of the uniform tilt angle. The theory showed [2] that at the transition from the *C** to the $\overline{C^*}$ phase the amplitude of the helicoidal part goes continuously to zero, while the tilt angle *and the helicoidal wave vector* remain finite and continuous through the transition. This is the type of continuous transition that has come to be known as an *instability transition*. This name derives from the fact that the coefficient of a quadratic term in the free energy changes sign as the transition is approached, and the free energy minimum corresponding to zero helicoidal amplitude at high temperatures becomes unstable. Michelson, Benguigui, and Cabib [2] found that in the *T*-*E* plane the line of second-order instability transitions should have a simple parabolic shape, at least for small E, as shown in Fig. 1(a). They soon realized, however, that coupling between the order parameter components would eventually lead to the quartic term becoming negative at lower temperatures and the transition becoming first order [3]. The point at which this changeover from second order to first order takes place is the tricritical point (TCP) indicated in the figure.

Somewhat later, other investigators [4–7] studied the *C** to $\overline{C^*}$ transition at much lower temperatures, far below the *A** to *C** transition. There the tilt angle may be assumed to be nearly independent of the field, and the nature of the transition is therefore quite different. It is much more in the nature of a field-unwinding transition, similar to what happens to a cholesteric liquid crystal in a magnetic field or to one with positive dielectric anisotropy in an electric field. At large fields the structure contains wide regions of nearly uniform tilt separated by narrow solitonlike regions of twist. The transition is also found to be continuous but now it is the *wave vector* of the helicoidal structure that goes to zero rather than its amplitude, which remains finite at the transition. This type of continuous transition has come to be known as a *nucleation* transition. This name derives from the fact that the reverse transition from the completely unwound

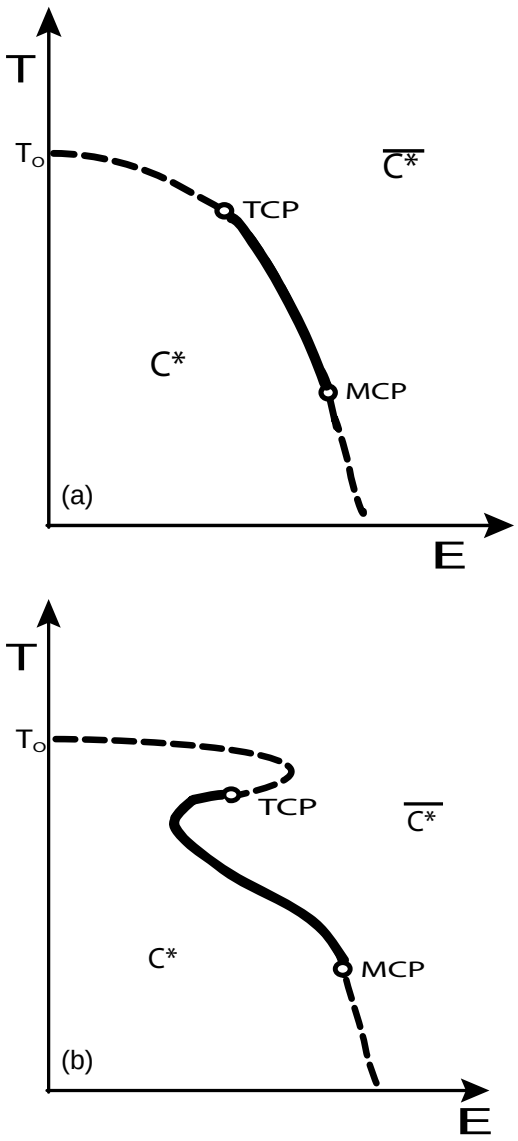

FIG. 1. *T*-*E* phase diagram according to (a) the simple Landau model [2,3,9] and (b) the extended Landau model [19–22]. Dashed (solid) lines are second- (first-)order transitions.

structure occurs through the spontaneous nucleation of twist solitons when the field is reduced below the critical unwinding value. De Gennes [8] appears to have been the first to clearly draw a distinction between instability and nucleation transitions; Schaub and Mukamel [9] were the first to apply these ideas to the C^* problem. In order to connect to the line of first-order transitions found for intermediate temperatures, as discussed above, there must be a *multicritcial* point (MCP), as first discussed by Schaub and Mukamel [9], where the transition changes back from first order to second order.

The line of first-order transitions must therefore change from being nucleation type at the MCP to instability type at the TCP. In between it should be of mixed character. From the experimental point of view the most distinguishing character of this line of first-order transitions would be that the *wave vector* of the helicoidal structure in the C^* phase at the transition should change from *zero* at the MCP to a *nonzero* value, nearly equal to that of the unperturbed helix, at the TCP. We stress this point since, as will be seen below, the observed behavior is quite different from this.

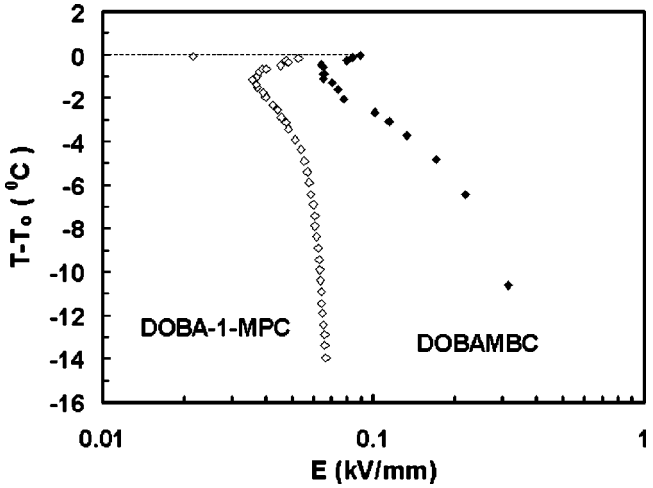

FIG. 2. *T*-*E* phase diagrams for DOBAMBC [10–15,17] and DOBA-1-MPC [16].

Soon after the theoretical studies of Michelson and Cabib, several experiments [10–17] were performed to investigate the effect of electric field on the helical structure of the C^* phase. These experiments were found to contradict the theoretical predictions in several respects. Most significantly, they showed that the phase transition temperature was not a quadratic function of E and was not even a monotonically decreasing function of E. This is illustrated in Fig. 2, which shows the C^* to $\overline{C^*}$ phase transition for two different compounds. Note that the abscissa has been changed to a logarithmic scale in order to accommodate the very different fields necessary to unwind these two different materials. The transition is seen to be *reentrant* for some range of fields so that by decreasing the temperature one could go from the C^* phase to the $\overline{C^*}$ phase and then presumably back to the C^* phase again. Closely related to this, most likely, was the observation that the helicoidal pitch, rather than being a constant as it would be in the theory of Michelson and Cabib and other models of that time, is also a nonmonotonic function of temperature, slowly rising to a maximum and then abruptly falling just before the transition to the A^* phase [12,13,15,18].

When these observations were made, it seemed that higher-order terms in the free energy expansion might be needed to accurately account for the reentrant behavior and the temperature dependence of the pitch, among other things. Accordingly a *generalized* Landau model, incorporating four additional higher-order terms, was introduced first in 1984 by Žekš [19] to account for the zero field results, and then subsequent to this Benguigui and Jacobs [20] and Kutnjak-Urbanc and Žekš [21] elaborated upon the model in an attempt to produce an explanation of the electric field effects. These later works showed, as illustrated in Fig. 1(b), that an S-shaped *T*-*E* phase diagram, at least qualitatively consistent with the experiments, could be produced.

Although it is conceivable that higher-order terms are im-

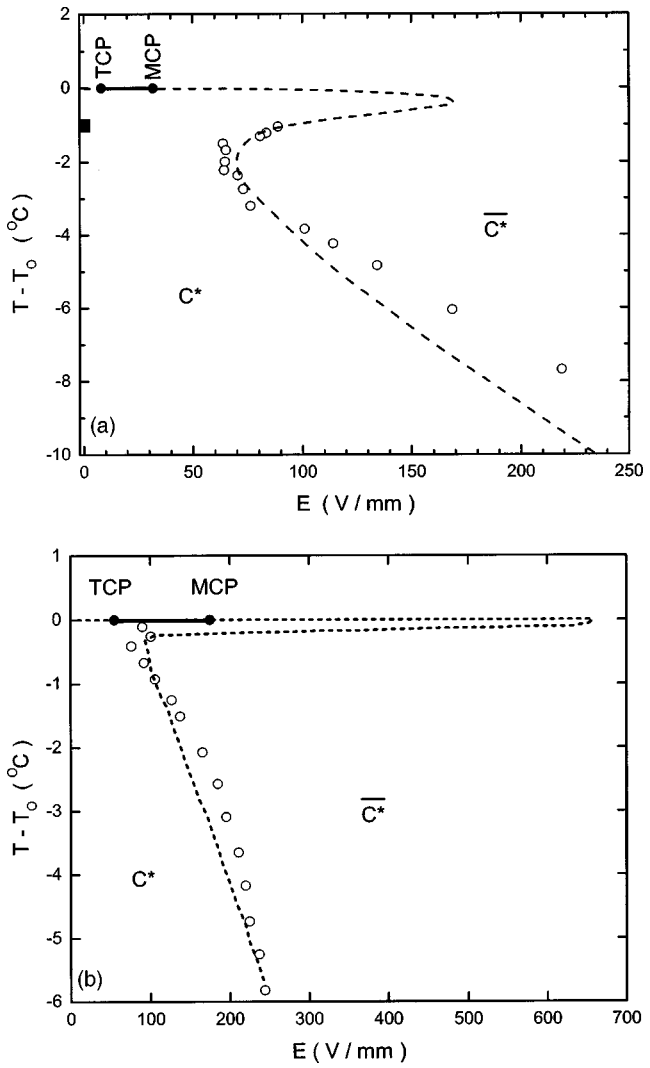

FIG. 3. *T-E* phase diagram of DOBAMBC with theoretical best fits of the extended Landau model according to (a) Benguigui and Jacobs [20] and (b) Kutnjak-Urbanc and Žekš [21]. TCP and MCP denote the predicted location in each case of the tricritical point and the multicritical point, respectively. Dashed (solid) lines are second- (first-)order transitions predicted by the theories.

portant, there are certain unsettling features concerning the approach that was used. First of all, not *all* possible higher terms of the same order were included, but only those four that could produce the desired effects. Second, the signs and coefficients of these four new terms could not assume any arbitrary values at all or else predicted behavior quite different from the observed would result. For example, in zero field the pitch as a function of temperature could have a maximum, as observed, but with different coefficients could also have a minimum, could monotonically increase or decrease, or could even change sign once or twice [22]. Finally, even when the coefficients were restricted to the values that correspond to observed data, reasonable fits could be obtained only by generating phase diagrams having transitions extending far into regions not corresponding to any observations. This last point is illustrated in Figs. 3(a) and 3(b), which show two different fits of the generalized Landau model to the data for *p*-decyloxybenzylidene *p′*-amino 2-methylbutylcinnamate (DOBAMBC). The first fit, due to Benguigui and Jacobs [20] and shown in Fig. 3(a), omits some of the lower-temperature data as well as the data point at zero field (shown as a solid black square in the figure). In other words, the zero on the ordinate misses the actual A^* to C^* transition—by about 1 °C as it turns out. The fit due to Kutnjak-Urbanc and Žekš [21], shown in Fig. 3(b), includes the zero field data point and this is what accounts for the extreme contortions of the S-shaped curve. It should be noted that for both of these fits the TCP and MCP are predicted to be on the very top, nearly horizontal part, of the S curve. All the experimental points, except for the zero field one, are thus predicted to correspond to continuous transitions of the nucleation type.

Remarkably, virtually all of the phase transition data presented up to now have been only for the lower S-curve part of the phase diagram. The data there are most easily taken by fixing the temperature and varying the electric field. Other regions of the phase diagram are best explored by fixing the field and varying the temperature, and this has not been done for the most part. One exception, of course, is the zero field data point, which has been found to be of the instability type. There is also one data point for *p*-decyloxybenzylidene *p′*-amino 2-methylpentylcinnamate (DOBA-1-MPC) taken by Kutnjak [16] shown just to the right of the zero field point in Fig. 2, but there is no indication of what type of transition corresponds to this one point. Generally a horizontal, or nearly horizontal, line has been drawn between the zero field data point and the highest-temperature data point to its right [10,16]. If the line were really horizontal then it would meet a smooth line going through the other data points at a sharp angle. The laws of thermodynamics would then indicate that there should be a third line of transitions to the right of this intersection, since no two transition lines may meet at an angle greater than 180°. This is the simplest expectation; alternately, and less likely in our opinion, there could be a greatly extended reentrant region as shown in Figs. 3(a) and 3(b) where there would be *two* successive transitions observed upon lowering or raising the temperature. Incredibly, there seem to have been no previous investigations in this area and this has served as one of the main motivations for the present work.

Moreover, a survey of the literature revealed that the most systematic studies of effects of electric field and temperature on the A^*-C^* and other phase transitions of a ferroelectric liquid crystal have been largely limited to DOBAMBC and its family members, such as DOBA-1-MPC. This raises the question as to whether the reentrant phenomena and other features of the phase diagram are universal or are limited to the DOBAMBC family and serves as another motivation for the present work. Thus we have selected the compound 4-(2′ methyl butyl) phenyl 4′-*n*-octylbiphenyl-4-carboxylate (CE8) belonging to a different chemical group for all of our studies and, as it turns out, have found behavior quite analogous to that found for the DOBAMBC family, suggesting that the phase diagram does have universal features.

Through visual observations, systematic measurements of intensity and tilt angle, and diffraction measurements of pitch as a function of both temperature and electric field, we

searched all regions of the C^* phase diagram and characterized all C^* phase transitions found as to their order and type. In the discussion section we shall organize and summarize our findings, which show that the T-E phase diagram is inadequately characterized by the existing theories.

Several of our measurements have been repeated on samples of different thicknesses. Almost all theoretical calculations thus far have addressed only the behavior of bulk materials, so there is a question as to whether or not finite sample thickness has some influence on experimental results.

EXPERIMENT AND RESULTS

The material used for the present study was the chiral liquid crystal 4-(2′ methyl butyl) phenyl 4′-*n*-octylbiphenyl-4-carboxylate. This liquid crystal has been reported [23] to have the phase sequence

Crystal 48 G^* 63.3 J^* 64.7 F^* 66.7 I^* 69 C^* 85 A^* 135 N^* 141 Iso,

where the numbers are the transition temperatures in °C. Between the N^* and isotropic phases, we found that there is also a narrow range of blue phase(s) not yet characterized. The existence of the N^* and blue phase(s) is one of the differences between this compound and the members of the DOBAMBC family.

The sample was prepared by filling the liquid crystal in an indium tin oxide (ITO) coated glass cell and was aligned in the bookshelf planar geometry. Mylar spacers were used to produce samples of three different thicknesses: 18, 90, and 230 μm. The electric field was applied parallel to the smectic layers and perpendicular to the helical axis. Prior to filling the cell, the ITO coated glass slides were cleaned thoroughly. To obtain a large homogeneously aligned area, we used the method outlined by Patel *et al.* [24] with some modifications. Good alignment was first obtained while the sample was in the A^* phase and then the temperature was lowered until the sample was in the C^* phase. The details of our procedure are given elsewhere [25].

The cell was placed in a temperature controlled hot stage, which was mounted on a Nikon polarizing microscope. Both visual observations as well as quantitative optical measurements were made. The data shown in Fig. 4, the phase diagram for the 18 μm cell, were acquired in both ways. For example, the data points on the curved portion of the diagram could be obtained by observing the change in texture as the C^* phase with its striped pattern converted to the virtually featureless $\overline{C^*}$ phase, or, since this change is accompanied by a sudden increase in intensity, they could also be obtained in that way. We found, however, that a more reliable and consistent method was to look for the disappearance of the diffraction from the sample, not by looking through the microscope eyepiece, but rather by looking at the hot stage by eye from the side. There one sees the full spectrum of diffracted light as long as the sample is in the periodic C^* phase, but when the voltage is increased and it changes to the $\overline{C^*}$ phase, the spectrum quickly goes away. In this manner the data shown in Fig. 4 for increasing voltage were produced. These results, which include a reentrant region, are quite similar to those of Fig. 2 although the electric fields are even larger for CE8. There is also a corresponding set of data for the case of decreasing voltages. The difference between the results for increasing versus decreasing voltage is a measure of the hysteresis and the first-order character of this transition [24].

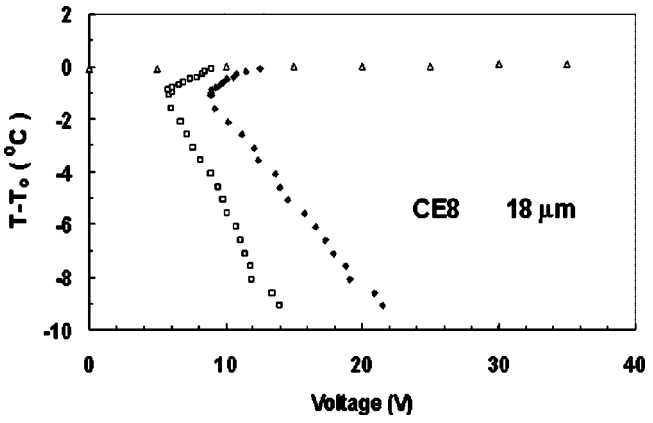

FIG. 4. T-E phase diagram of CE8, 18 μm cell thickness. Triangles are for data taken via temperature scans. Diamonds and squares are, respectively, for increasing and decreasing voltage scans.

The other data points on the phase diagram of Fig. 4, observed to be almost a horizontal line, were all acquired by the use of temperature scans. The $\overline{C^*}$-C^* transition starting from zero field (where it is actually an A^*-C^* transition) may also be detected by the several methods discussed above. All these procedures, including observations of texture changes, intensity changes, and appearance or disappearance of diffraction effects, give consistent results. These observations are also completely temperature reversible, showing no noticeable hysteresis, thus indicating that this transition is second order. The fact that the diffraction in the C^* phase persists right up to the beginning of the $\overline{C^*}$ phase shows that this is a transition of the instability type.

We find that this $\overline{C^*}$-C^* transition line is indeed horizontal as has been suggested before, although now we have many more data (see also Fig. 7 below) to support this claim. As mentioned earlier, the fact that this horizontal line meets the other C^*-$\overline{C^*}$ transition line at a sharp angle really requires that there be another transition line extending to the right beyond the intersection of these two lines. We have investigated this region for such a transition and have found strong indications that one exists. The evidence is not as extensive as for the other transitions since there is no diffraction from either phase and the textures of both phases are

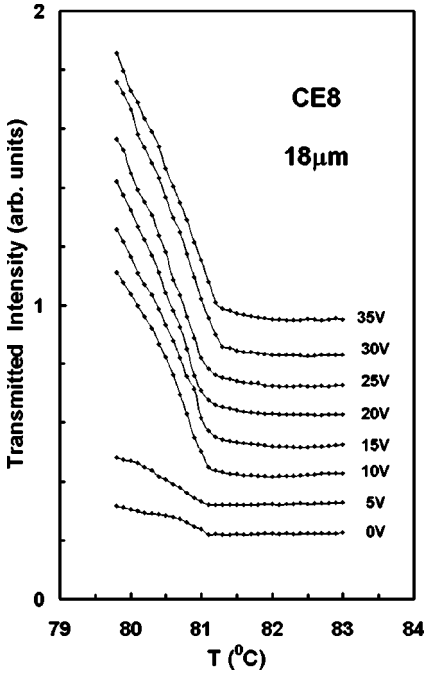

FIG. 5. Transmitted intensity vs temperature for CE8, 18 μm cell thickness. The transition temperature is about 81 °C.

nearly featureless. Nevertheless, there is a sudden rise in intensity at the purported transition and, furthermore, the slope of this rise is even greater than for the temperature scans for the $\overline{C^*}$-C^* transition, as is shown in Fig. 5. Additional quantitative evidence for the transition comes from measurements of the tilt angle, given in Fig. 6. The tilt angle has been measured in the usual way: the extinction angles for both polarities of the applied field were measured and the tilt angle was taken to be half of their difference. The tilt angle data, as expected, mirror the intensity data. Both show small pretransitional increases at the high-temperature side (T_c $=81\,^{\circ}$C) because of the electroclinic effect on the A^* phase, while on the low-temperature side there is a large increase presumably because of an instability transition. There is no apparent hysteresis to this transition, which therefore appears to be of second order. We leave aside until the Discussion section the important questions as to how there could be a transition in this region in the first place and what its nature would be.

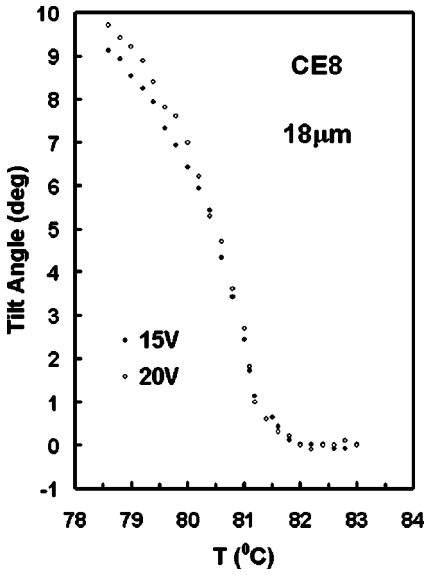

FIG. 6. Tilt angle vs temperature for CE8, 18 μm cell thickness. The transition temperature is about 81 °C.

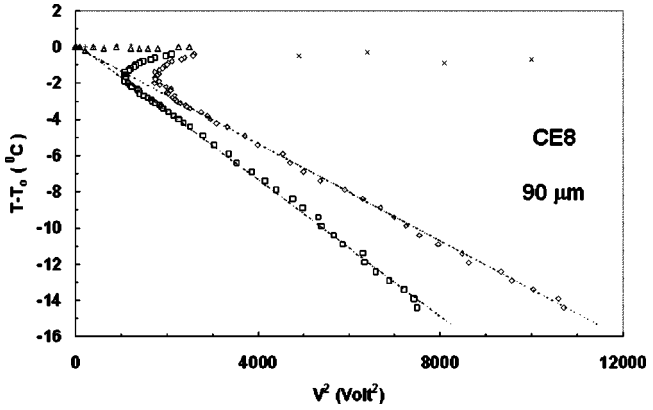

FIG. 7. T-V^2 phase diagram of CE8, 90 μm cell thickness. The dashed lines are guides to the eye illustrating the linear behavior at lower temperatures.

In Fig. 7 we show the results of similar studies performed on the 90 μm thick sample cell. To within our experimental uncertainties it appears that the voltages scale with the sample thickness, as expected. In this figure we have plotted the data as temperature versus voltage squared to illustrate an interesting result that does not seem to have been noticed before. The lower-temperature data may be seen to follow a quite linear trend, which, moreover, extrapolates precisely to the zero field A^*-C^* point. So, in this region, the phase boundary does have the simple parabolic shape that the earliest theories had predicted. This gives some hope that there might ultimately be a simple theory of the phase diagram.

For quantitative diffraction measurements the sample and hot stage were removed from the microscope stage and placed on a freestanding horizontal stage. A 5 mW HeNe laser shone vertically downward, perpendicular to the sample, while a horizontal linear photodiode array placed beneath the sample detected the locations and intensities of the diffraction peaks. For laser polarizations parallel and perpendicular to the helical axis the locations of the diffraction peaks were slightly different, an effect for which we have no simple explanation. The diffraction intensities were much stronger for the polarization perpendicular to the helix (parallel to the smectic layers), and all of the data reported here were taken in this way.

With our diffraction setup we determined the pitch of the sample as a function of both temperature and voltage. The behavior of the pitch as a given phase transition is approached provides an important clue as to whether the transition is more like an instability type or more like a nucleation type.

Figure 8 shows the pitch versus temperature for the 90 μm sample in the absence of any applied voltage. The slow

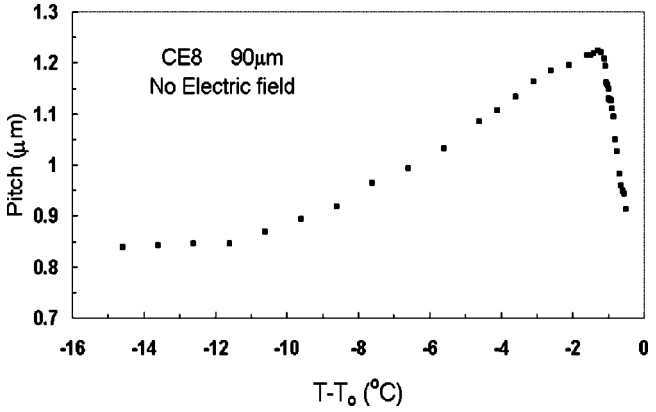

FIG. 8. Pitch vs temperature for CE8, 90 μm cell thickness.

rise of the pitch with temperature followed by the dramatic drop just before the transition to the A^* phase are similar to what has been seen for every other C^*-A^* transition both in the DOBAMBC family and elsewhere. In spite of these large swings, the pitch remains finite at the transition, indicating again that this second-order transition is of the instability type. This remains true even for applied fields right up to the intersection with the other phase boundary, which is first order.

We note that our measured pitch values, typically about 1 μm, are in good agreement with those reported by Drevenšek *et al.* [26] but are one-third as large as reported even earlier for CE8 [27,28]. These earlier studies used methods less direct than diffraction and were evidently in error. Unfortunately, because of this confusion we mistakenly referred to CE8 as a ''large pitch'' material in an earlier publication [25].

The voltage dependence of the pitch for various fixed temperatures is shown in Fig. 9. For all temperatures the pitch is a monotonically increasing function of voltage. In some respects this unwinding of the helix is like a nucleation transition, but it cannot be called one since the transition is first order and the unwinding is incomplete. We note, however, that the unwinding is closer to being complete at the

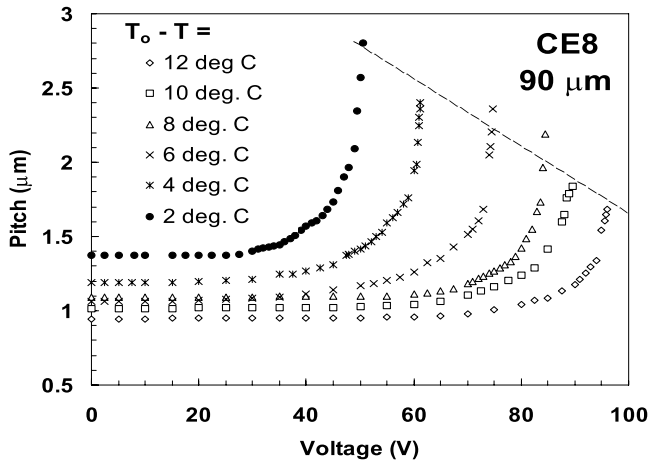

FIG. 9. Pitch vs voltage for CE8, 90 μm cell thickness. The dashed line is a guide to the eye.

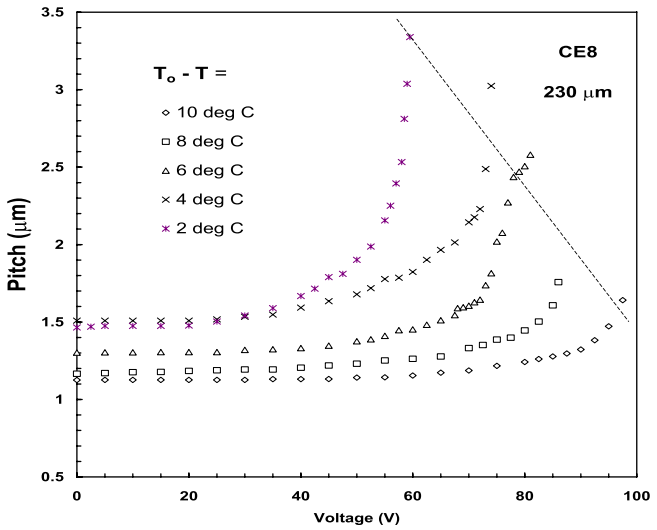

FIG. 10. Pitch vs voltage for CE8, 230 μm cell thickness.

higher temperatures, as shown by the dashed line in the figure.

Figure 10 shows similar data taken for the 230 μm cell. Not unsurprisingly, the quality of the data is not as good as for the thinner cell, for which it is much easier to get good alignment. The data are good enough, however, to see that at any given temperature the unwinding is about 10% more complete in this cell, which is about two and one-half times thicker. The difference is not large enough to suggest that the unwinding would be complete in a bulk material, except perhaps at the highest temperatures.

DISCUSSION

The experimental results presented here are easily seen to be completely incompatible with any of the theoretical proposals that have been advanced for the phase transformations of the C^* phase. For example, if the results were to follow either of the proposed phase diagrams of Fig. 2, then there should be a first-order transition region along the horizontal section between the TCP and the MCP, but none has been seen. Also, the transition would be expected to be continuous along the curved portion of the diagram, but it is decidedly discontinuous. In order to salvage the theories, one might propose that the point separating the continuous horizontal portion from the first-order curved portion is the postulated TCP, but this suggestion is also seen to be incompatible with the theory. For them the MCP must lie at still lower temperatures and the wave vectors at the discontinuous transition should become smaller at the lower temperatures, whereas they are actually seen to become larger. Finally, it goes without saying that the additional horizontal phase boundary we have proposed extending far to the right is not predicted at all, although it would seem to be required if thermodynamics laws are to apply. Although previous experiments have not explored the phase diagram as thoroughly as we have, they do seem to be consistent with our findings. Thus there is reason to believe that there is a universal phase diagram for these transitions, although one that is very different from the theoretical predictions.

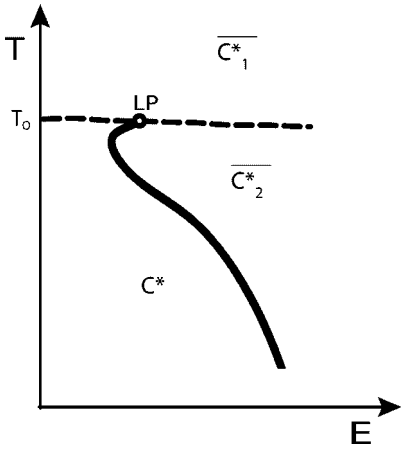

FIG. 11. Proposed T-E phase diagram for the C^* phase. Dashed (solid) lines are second- (first-)order transitions. LP denotes the Lifshitz point.

Based upon our experimental findings, and symmetry requirements as well, we present the phase diagram in Fig. 11 as the simplest proposal that is compatible with the experimental observations. It has no points with the characteristics of either the TCP or the MCP previously proposed, but instead has another type of multicritical point. It is in fact very similar in appearance to theoretical proposals for the behavior of this same system in a *magnetic* field [21,29–31], although the phases must obviously have different symmetries in the two cases. In both cases there are two mostly horizontal lines of second-order transitions meeting a curved vertically rising line of first-order transitions at a triple point. This triple point in the magnetic case is a special kind of multicritical point called a Lifshtiz point (LP) [29] and so we tentatively refer to it as such in our case as well. In the magnetic case the highest-temperature phase is the A^* phase, whereas in the electric case it is a $\overline{C^*}$ phase. However, the ''unwound'' phase appearing in the lower right side of the diagram is also a $\overline{C^*}$ phase and so we refer to it as $\overline{C^*_2}$ and to the upper $\overline{C^*}$ phase as $\overline{C^*_1}$, as indicated in the figure. A possibility for the symmetry difference between these two $\overline{C^*}$ phases will be discussed below.

If both horizontal transition lines are indeed second order, then it must be the case that the first-order line meeting them at the LP also becomes second order at the LP. In other words, the unwinding of the C^* phase by the field, which we have found to be incomplete but more nearly complete at higher temperatures, must become fully complete at the LP. Thus the C^*-$\overline{C^*_2}$ transition finally becomes a transition of the nucleation type at the LP *only*.

The C^*-$\overline{C^*_1}$ transition is an instability type transition but now it must be the case that the finite wave vector at the transition approaches zero as the LP is approached. Thus the C^*-$\overline{C^*_1}$ instability transition becomes simultaneously a nucleation transition at the LP.

Since there is no wave vector associated with either the $\overline{C^*_1}$ or the $\overline{C^*_2}$ phase, the transition between them must be of an instability type. What then is the nature of this instability and what is the symmetry difference between these two phases? Although we are uncertain of the answers to these questions, one possibility seems plausible. We conjecture that this transition involves a change in the *tilt* of the molecules. We recall that when a dc electric field is applied to an A^* phase, the electroclinic effect produces a lilt that is exactly *perpendicular* to the applied field. We speculate that in the $\overline{C^*_2}$ phase the molecules acquire a component of tilt along the field direction also. Now this can certainly happen if the polarizability of the molecules is considered, that is, if one includes the usual quadratic coupling of the field to the orientational order parameter, a term that has been left out in all previous theoretical calculations of the phase diagram, to our knowledge. This term has undoubtedly been omitted because it was anticipated that at higher temperatures the fields would be weak enough that only the linear coupling to the field, the electroclinic effect, needed to be included. But experience has shown that even at these higher temperatures the experimental fields can be large and so this term needs to be considered. Note that this quadratic term *has* been included, however, for lower temperatures, where it is expected that large fields will be needed to unwind the helix [4–7]. It has also been incorporated into the theory for the magnetic case [21,29–31] because there it is the lowest-order field coupling term.

Finally, we remark that when such large fields are involved there must be notable biaxiality present and so the full tensor orientational order parameter might be needed rather than the simple two component Pikin-Indenbom parameter [32] that has mostly been used.

ACKNOWLEDGMENT

This work was supported in part by the National Science Foundation through Grant No. DGE-9870720.

[1] R.B. Meyer, L. Liebert, L. Strzelecki, and P. Keller, J. Phys. (France) Lett. **36**, L69 (1975).
[2] A. Michelson, L. Benguigui, and D. Cabib, Phys. Rev. A **16**, 394 (1977).
[3] A. Michelson and D. Cabib, J. Phys. (France) Lett. **38**, L321 (1977).
[4] V.E. Dmitrienko and V.A. Belyakov, Sov. Phys. JETP **51**, 787 (1981).
[5] Ph. Martinot-Lagarde, Mol. Cryst. Liq. Cryst. **66**, 61 (1981).
[6] O. Hudak, J. Phys. (France) **44**, 57 (1983).
[7] M. Yamashita, Prog. Theor. Phys. **74**, 622 (1985).
[8] P.G. de Gennes, in *Fluctuations, Instabilities, and Phase Transitions*, Vol. 11 of *NATO Advanced Study Institute, Series B: Physics*, edited by T. Riste (Plenum, New York, 1975).
[9] B. Schaub and D. Mukamel, J. Phys. C **16**, L225 (1983).
[10] H. Takezoe, K. Furuhata, T. Nakagiri, A. Fukuda, and E. Kuze, Jpn. J. Appl. Phys. **17**, 1219 (1978).
[11] K. Kondo, H. Takezoe, A. Fukuda, and E. Kuze, Jpn. J. Appl.

Phys., Part 2 **22**, L43 (1983).
[12] H. Takezoe, K. Kondo, K. Miyasato, S. Abe, T. Tsuchiya, A. Fukuda, and E. Kuze, Ferroelectrics **58**, 55 (1984).
[13] S.A. Rozanski and W. Kuczynski, Chem. Phys. Lett. **105**, 104 (1984).
[14] S. Dumrongrattana and C.C. Huang, J. Phys. (France) **47**, 2117 (1986).
[15] A. Ezcurra, M.A. Perez Jubindo, M.R. De La Fuente, J. Etxebarria, A. Remon, and M.J. Tello, Liq. Cryst. **4**, 125 (1989).
[16] Z. Kutnjak, M.S. thesis, University of Ljubljana, 1991.
[17] A. Levstik, Z. Kutnjak, B. Žekš, S. Dumrongrattana, and C.C. Huang, J. Phys. II **1**, 797 (1991).
[18] I. Muševič, B. Žekš, R. Blinc, L. Jansen, A. Seppen, and P. Wyder, Ferroelectrics **58**, 71 (1984).
[19] B. Žekš, Mol. Cryst. Liq. Cryst. **114**, 259 (1984).
[20] L. Benguigui and A.E. Jacobs, Phys. Rev. E **49**, 4221 (1994).
[21] B. Kutnjak-Urbanc and B. Žekš, Phys. Rev. E **51**, 1569 (1995).
[22] T. Carlsson, B. Žekš, C. Filipič, A. Levstik, and R. Blinc, Mol. Cryst. Liq. Cryst. **163**, 11 (1988).
[23] H. Stegemeyer, R. Meister, U. Hoffman, and W. Kuczynski, Liq. Cryst. **10**, 295 (1991).
[24] J.S. Patel, T.M. Leslie, and J.W. Goodby, Ferroelectrics **59**, 137 (2002).
[25] F. Ghoddoussi, M. Pantea, P.H. Keyes, R. Naik, and P.P. Vaishnava, Ferroelectrics **278**, 13 (2002).
[26] I. Drevenšek, I. Muševič, and M. Čopič, Phys. Rev. A **41**, 923 (1990).
[27] M.F. Bone, D. Coates, and A.B. Davey, Mol. Cryst. Liq. Cryst. **102**, 331 (1984).
[28] G. Spruce and R.D. Pringle, Liq. Cryst. **3**, 507 (1988).
[29] A. Michelson, Phys. Rev. Lett. **39**, 464 (1977).
[30] L. Benguigui and A.E. Jacobs, Ferroelectrics **84**, 379 (1988).
[31] A.E. Jacobs and L. Benguigui, Phys. Rev. A **39**, 3622 (1989).
[32] V. L. Indenbom, S.A. Pikin, and E.B. Loginov, Sov. Phys. Crystallogr. **21**, 632 (1976).